

Study of the pseudoscalar glueball in J/ψ radiative decays

Long-Cheng Gui^{1,2,3,*}, Ying Chen^{4,5,†}, Jia-Mei Dong¹, and Yi-Bo Yang^{6,‡}

¹*Department of Physics, Hunan Normal University, Changsha, Hunan, China*

²*Key Laboratory of Low-Dimensional Quantum Structures and Quantum Control of Ministry of Education, Changsha 410081, China*

³*Synergetic Innovation Center for Quantum Effects and Applications(SICQEA), Hunan Normal University, Changsha 410081, China*

⁴*Institute of High Energy Physics, Chinese Academy of Sciences, Beijing 100049, China*

⁵*School of Physics, University of Chinese Academy of Sciences, Beijing 100049, China*

⁶*Institute of Theoretical Physics, Chinese Academy of Sciences, Beijing 100190, China*

We aim to explore the production rate of the pseudoscalar glueball in J/ψ radiative decay by lattice QCD in quenched approximation. The calculation is performed on three anisotropic lattices with the spatial lattice spacing ranging from 0.222(2) fm to 0.110(1) fm. As a calibration of some systematical uncertainties, we first extract the $M1$ form factor $\hat{V}(0)$ of the process $J/\psi \rightarrow \gamma\eta_c$ and get the result $\hat{V}(0) = 1.933(41)$ in the continuum limit, which gives the partial width $\Gamma(J/\psi \rightarrow \gamma\eta_c) = 2.47(11)$ keV. These results are in agreement with that of previous lattice studies. As for the pseudoscalar glueball G_{0-+} , its mass is derived to be 2.395(14) GeV, and the form factor $V(0)$ of the process $J/\psi \rightarrow \gamma G_{0-+}$ is determined to be $\hat{V}(0) = 0.0246(43)$ after continuum extrapolation. Finally, the production rate of the pseudoscalar glueball is predicted to be $2.31(90) \times 10^{-4}$, which is much smaller than that of conventional light $q\bar{q}$ η states. After the subtraction of the phase space factor, the couplings of $J/\psi X\gamma$ are similar where X stands for η states and the pseudoscalar glueball. Possibly, the $U_A(1)$ anomaly plays an important role for the large couplings of gluons to the flavor singlet η states in J/ψ radiative decays.

PACS numbers: 11.15.Ha, 12.38.Gc, 12.39.Mk, 13.25.Gv

I. INTRODUCTION

Quantum chromodynamics (QCD) predicts the existence of glueballs, namely, the bound states of gluons. Last several decades witnessed the intensive and extensive investigations of glueballs both in experiments and theoretical studies[1–11]. Experimentally, there are ten scalar mesons observed with approximately degenerated masses around 1.5 GeV, among which $f_0(1370)$, $f_0(1500)$, and $f_0(1710)$ are the three isoscalars. According to the quark model, if these states can be sorted into the $q\bar{q}$ $SU(3)$ nonet, then the surplus one isoscalar hints the existence of an additional degree of freedom, possibly a glueball states, which can be either one of the isoscalars mentioned above, or mixes with the conventional $q\bar{q}$ states. A similar consideration applies to the pseudoscalar channel: the three isoscalar pseudoscalar mesons $\eta(1295)$, $\eta(1405)$, and $\eta(1495)$ also motivates the conjecture of the existence of a pseudoscalar glueball in this mass range. Actually, there are many phenomenological studies assigning $\eta(1405)$ to be the most likely candidate for the pseudoscalar glueball due to its large production fraction in the J/ψ radiative decays. However, this assignment has tensions with the prediction of the pseudoscalar glueball mass from lattice QCD.

Lattice QCD is the ab initio nonperturbative approach

for solving QCD and plays a key role in the investigation of the low energy strong interaction phenomena. In the glueball sector, lattice QCD in the quenched approximation predicts that the masses of the lowest lying scalar, tensor and pseudoscalar glueballs are roughly 1.5 – 1.7 GeV, 2.2 – 2.4 GeV, and 2.6 GeV, respectively[1, 2]. Recent lattice calculations with dynamical quarks seemingly support these predictions and do not observe large unquenched effects[4, 5]. As far as the pseudoscalar glueball is concerned, its predicted mass, say, around 2.6 GeV, is much higher than that of $\eta(1405)$. This discrepancy cannot be easily mediated by considering the glueball-meson mixing in the presence of dynamical quarks. It is interesting to notice that some phenomenological studies advocate $\eta(1405)$ and $\eta(1495)$ be the same state which appears differently in different final states due to some dynamical mechanism[12]. If this is the case, then there is no redundant pseudoscalar meson mass region and subsequently no need for an additional degree of freedom such as a glueball in 1.5 GeV mass region. As such, one may wish to search for the pseudoscalar glueball in the energy range beyond 2 GeV according to the lattice predictions.

J/ψ radiative decays are regarded as an important hunting ground for glueballs, owing to its the gluon-rich environment and cleaner background. Apart from their masses, the production rates of glueballs in J/ψ radiative serve as additional key criteria for the identification of glueballs, if they can be derived reliably from the theoretical calculation. Also some quenched lattice QCD efforts have been made to calculate these production rates of the scalar and tensor glueballs [13, 14]. Since

* guilongcheng@hunnu.edu.cn

† cheny@ihep.ac.cn

‡ ybyang@itp.ac.cn

the pure gauge glueballs are well defined hadron states in the quenched approximation, the electromagnetic form factors of J/ψ radiatively decaying into glueballs can be extracted directly by calculating the matrix elements of the electromagnetic current between J/ψ and glueballs. With these form factors, the branch fraction of J/ψ radiative decaying into the pure gauge scalar glueball is predicted to be $3.8(9) \times 10^{-3}$. It is interesting to notice that the sum of the observed branching fraction of the processes $J/\psi \rightarrow \gamma f_0(1710) \rightarrow \gamma + \text{anything}$ gives a value of roughly 2.0×10^{-3} which is very close to the above predicted value for the pure gauge glueball, while that of $J/\psi \rightarrow \gamma f_0(1500)$ is an order of magnitude smaller.

Recently, the BESIII collaboration has performed the partial wave analysis to the process $J/\psi \rightarrow \gamma \phi \phi$ and observed a new resonance $X(2500)$ with the resonance parameters $M_X = 2470_{-19-23}^{+15+101}$ and $\Gamma_X = 230_{-35-33}^{+64+56}$ [15]. In the process $J/\psi \rightarrow \gamma \eta' \pi^+ \pi^-$, BESIII observed a complicated structure in the $\eta' \pi^+ \pi^-$ invariant mass spectrum and reported two new resonances $X(2120)$ and $X(2370)$, whose quantum number are likely $J^{PC} = 0^{-+}$ [16]. These new resonances lie in the mass range of the pseudoscalar glueball predicted by lattice QCD and are worthy of further experimental investigations. However, in order to unravel the nature of these states, more theoretical inputs are desired.

In this work, we calculate the production rate of the pseudoscalar glueball from lattice QCD by adopting the similar strategy in the scalar and tensor cases. Even though that the dynamical lattice QCD simulation is dominant nowadays, the study of glueballs is still challenging since it requires much higher statistics comparing to the usual hadron. Therefore, we would like to perform exploratory investigation by generating the quenched gauge configurations with large statistics using the anisotropic lattices. In order to calibrate part of uncertainties, we first calculate the partial width of the process $J/\psi \rightarrow \gamma \eta_c$ and compare with the results of previous lattice calculations and experiments. We admit that glueballs may have strong mixing with conventional mesons in the real world, and then the quenched effects on our result of glueball production rates cannot be reliably estimated in the present stage.

This work is organized as follows: Section 2 mainly introduces the calculation formulism of radiative transition width on lattice QCD. Section 3 presents the calculation details and results, including the parameters of the lattice, the relevant quality spectrum, and transition form-factors. We give the conclusion and some discussion in Section 4.

II. FORMALISM

Generally speaking, the partial decay width of J/ψ radiatively decaying into a pseudoscalar meson X can be

calculated through the following formula,

$$\Gamma_{J/\psi \rightarrow \gamma X} = \frac{1}{24\pi} \frac{|\vec{q}|}{M_{J/\psi}^2} \sum_{\lambda_{J/\psi}, \lambda_\gamma} |\mathcal{M}_{\lambda_{J/\psi}, \lambda_\gamma}(\vec{p}_i, \vec{p}_f)|^2, \quad (1)$$

where \vec{p}_i and \vec{p}_f are the momenta of J/ψ and X , respectively, $\vec{q} = \vec{p}_i - \vec{p}_f$ is the decaying momentum of the emitted photon in the rest frame of J/ψ , $\lambda_{J/\psi}$ and λ_γ stand for the different polarizations of J/ψ and the photon, and $\mathcal{M}_{\lambda_{J/\psi}, \lambda_\gamma}$ is the on-shell transition amplitude. The magnitude q can be defined through the masses of J/ψ (denoted by $M_{J/\psi}$) and X (denoted by M_X), say, $|\vec{q}| = \frac{M_{J/\psi}^2 - M_X^2}{2M_{J/\psi}}$. The transition amplitude contains all the dynamics of the decay, and can be expressed to the lowest order of QED as

$$\mathcal{M}_{\lambda_{J/\psi}, \lambda_\gamma} = \epsilon_\mu^*(\vec{q}, \lambda_\gamma) \langle X(\vec{p}_f) | J_{\text{em}}^\mu | J/\psi(\vec{p}_i, \lambda_{J/\psi}) \rangle, \quad (2)$$

where $\epsilon_\mu^*(\vec{q}, \lambda_\gamma)$ is the polarization vector of photon and $J_{\text{em}}^\mu = \sum_f e_f \bar{\psi}_f \gamma^\mu \psi_f$ is the relevant electromagnetic vector current with the summation over all possible quark flavors. If the sea quark contributions through disconnected diagrams can be neglected, one can use $J_{\text{em}}^\mu = e_c \bar{c} \gamma^\mu c$ as an approximation for the electromagnetic decays of charmonia. Usually, the matrix elements $\langle X(\vec{p}_f) | J_{\text{em}}^\mu(0) | J/\psi(\vec{p}_i, \lambda_{J/\psi}) \rangle$ can be expressed in terms of form factor through the multipole decomposition. For the pseudoscalar X , the explicitly expression is

$$\langle X(\vec{p}_f) | J_{\text{em}}^\mu(0) | J/\psi(\vec{p}_i, \lambda_{J/\psi}) \rangle = M(Q^2) \epsilon^{\mu\nu\rho\sigma} P_{i,\nu} P_{f,\rho} \times \epsilon_\sigma(\vec{p}_i, \lambda_{J/\psi}) \quad (3)$$

where $Q^2 \equiv -(P_i - P_f)^2$ and $M(Q^2)$ is the multipole form factor, which is sometimes also expressed in terms of a dimensionless form factor $V(Q^2)$ as $M(Q^2) = \frac{2V(Q^2)}{m_X + m_{J/\psi}}$. Thereby the partial decay width can be written as

$$\begin{aligned} \Gamma_{J/\psi \rightarrow \gamma X} &= \frac{1}{12\pi} |\vec{q}|^3 |M(0)|^2 \\ &\equiv \frac{1}{3\pi} \frac{|\vec{q}|^3}{(m_{J/\psi} + m_X)^2} |V(0)|^2. \end{aligned} \quad (4)$$

It is clearly seen that if the matrix elements in Eq. (3) are known, the form factor $M(Q^2)$ (or equivalently $V(Q^2)$) can be derived to give the decay width directly. Actually, this goal can be achieved in lattice QCD study by calculating the relevant three-point correlation functions

$$\begin{aligned} \Gamma_{J/\psi \rightarrow \gamma X}^{(3), \mu i}(\vec{p}_i, t_i; \vec{p}_f, t_f; t) &= \sum_{\vec{x}, \vec{y}, \vec{z}} e^{-i\vec{p}_i \cdot \vec{x}} e^{i\vec{q} \cdot \vec{y}} e^{-i\vec{p}_f \cdot \vec{z}} \\ &\quad \langle \mathcal{O}_X(\vec{z}, t_f) J_{\text{em}}^\mu(\vec{y}, t) \mathcal{O}_{J/\psi, i}^\dagger(\vec{x}, t_i) \rangle, \end{aligned} \quad (5)$$

where \mathcal{O}_X and $\mathcal{O}_{J/\psi, i}$ are interpolating field operators for X and J/ψ , respectively. After the intermediate state insertion, the three-point function $\Gamma_{J/\psi \rightarrow \gamma X}^{(3), \mu i}$ is parameterized as

$$\begin{aligned}
\Gamma_{J/\psi \rightarrow \gamma X}^{(3),\mu i}(\vec{p}_i, t_i; \vec{p}_f, t_f; t) &= \sum_{m,n,\lambda_n} \frac{e^{-E_m t_f} e^{-(E_n - E_m)t}}{4E_m E_n} \langle \Omega | \mathcal{O}_f(0) | m, \vec{p}_f \rangle \\
&\times \langle m, \vec{p}_f | J_{em}^\mu(0) | n, \vec{p}_i, \lambda_n \rangle \langle n, \vec{p}_i, \lambda_n | \mathcal{O}_{J/\psi, i}^\dagger(0) | \Omega \rangle \\
\stackrel{t_f \gg t \gg 0}{\rightarrow} &\frac{e^{-E_X t_f} e^{-(E_{J/\psi} - E_X)t}}{4E_{J/\psi} E_X} Z_i^{*(J/\psi)} Z^{(X)} \langle X(\vec{p}_f) | J_{em}^\mu(0) | J/\psi(\vec{p}_i, \lambda_{J/\psi}) \rangle
\end{aligned} \tag{6}$$

where E_X and $E_{J/\psi}$ are the energies of X and J/ψ , respectively, $Z_i^{(J/\psi)} = \langle J/\psi(p_f, \lambda_{J/\psi}) | \mathcal{O}_{J/\psi, i}(0) | \Omega \rangle$, and $Z^{(X)} = \langle X(p_f) | \mathcal{O}_X(0) | \Omega \rangle$, which can be extracted from the relevant two-point functions

$$\begin{aligned}
\Gamma_{ij}^{(2)}(\vec{p}, t) &= \sum e^{-i\vec{p}\cdot\vec{x}} \langle \Omega | \mathcal{O}_i(\vec{x}, t) \mathcal{O}_j^\dagger(0, 0) | \Omega \rangle \\
\stackrel{t \rightarrow \infty}{\rightarrow} &\frac{Z_i Z_j^*}{2E(\vec{p})} e^{-E(\vec{p})t}.
\end{aligned} \tag{7}$$

Practically, one can carry out a joint fit to the two-point functions and the three-point function to extract the desired matrix elements in Eq. (3), from which the multipole form factors can be derived at different Q^2 .

III. NUMERICAL DETAILS

As addressed in Sec. I, we perform the calculation in the quenched approximation. Since J/ψ , η_c , and the pseudoscalar glueball are heavy particles, in order to obtain good signals with high resolutions in the temporal direction, we generate the gauge configurations on anisotropic lattices with the temporal lattice much finer than the spatial lattice, say, $\xi = a_s/a_t \gg 1$, where a_s and a_t are the spatial and temporal lattice spacings, respectively. In practice, we choose $\xi = 5$. The gauge action we use is the tadpole improved gauge action [17] whose discretization error is expected to be $O(a_s^4, \alpha_s a_s^2)$. Three gauge ensembles with large statistics are generated at different lattice spacings for the continuum extrapolation, and the relevant ensemble parameters are listed in Tab. I, where the lattice spacings a_s are determined from $r_0^{-1} = 410(20)$ MeV by calculating the static potential. For fermions, we use the tadpole improved clover action for anisotropic lattices [18]. The parameters in the action are tuned carefully by requiring that the physical dispersion relations of vector and pseudoscalar mesons are correctly reproduced at each bare quark mass [19]. The bare charm quark masses for the two lattices are set by the physical mass of J/ψ , $m_{J/\psi} = 3.097$ GeV.

In the quenched approximation, since there are no sea quarks, the electromagnetic current contributing to the radiative transitions of charmonia involves only the charm quark, say, $j_{em}(x) = Q_c j^\mu(x)$ with $j^\mu(x) = \bar{c}\gamma_\mu c(x)$, which is the one we adopt in this study. It is a conserved vector current and need not be renormalized in the continuum. However, on a finite lattice, it is not conserved anymore due to the lattice artifact and receives a multiplicative renormalization factor $Z_V(a_s)$. Following the scheme proposed by Ref. [20], $Z_V(a_s)$ is extracted us-

TABLE I. Relevant input parameters for this work. The spatial lattice spacing a_s is determined from $r_0^{-1} = 410(20)$ MeV by calculating the static potential.

β	ξ	a_s (fm)	La_s (fm)	$L^3 \times T$	$N_{conf.}$
2.4	5	0.222(2)	1.78	$8^3 \times 96$	20000
2.8	5	0.138(1)	1.66	$12^3 \times 144$	20000
3.0	5	0.110(1)	1.76	$16^3 \times 160$	10000

TABLE II. The renormalization constants $Z_V^{(s)}$ and $Z_V^{(t)}$ of the spatial and temporal components of the vector current for $\beta = 2.4$, $\beta = 2.8$ and $\beta = 3.0$ lattices. Two momentum modes, (0,0,0) and (1,0,0), are used for the derivation.

β	$Z_V^{(t)}(0,0,0)$	$Z_V^{(t)}(1,0,0)$	$Z_V^{(s)}(1,0,0)$
2.4	1.288(5)	1.299(11)	1.388(15)
2.8	1.155(3)	1.159(3)	1.110(7)
3.0	1.106(4)	1.114(6)	1.062(6)

ing the ratio of the η_c two-point function and the related three-point function evaluated at $Q^2 = 0$,

$$Z_V^{(\mu)}(t) = \frac{p^\mu}{E(\vec{p})} \frac{1}{2} \Gamma_{\eta_c}^{(2)}(\vec{p}; t_f = \frac{n_t}{2}), \tag{8}$$

where the factor 1/2 accounts for the effect of the temporal periodic boundary condition, and the superscript μ of $Z_V(a_s)$ is used to differentiate the temporal component from the spatial ones, since they are not necessarily the same due to the anisotropic lattices we used. Fig. 1 plots $Z_V^{(\mu)}(t)$ with respect to t for the three lattices. Z_V 's are extracted from the plateaus and the values are listed in Tab. II. Obviously, the spatial components $Z_V^{(s)}(a)$ deviate from the temporal ones by a few percent. This deviation can be attributed to the imperfect tuning of the bare velocity in the fermion action. In this work, only $Z_V^{(s)}$'s enter the calculation since only the spatial components of the vector current are involved in the extraction of the form factors.

A. $J/\psi \rightarrow \gamma \eta_c$ transition

There have been quite a few lattice studies on the decay process $J/\psi \rightarrow \gamma \eta_c$. We would like to carry the similar calculation and make a comparison with previous studies as well as the experimental value, which serve as a calibration to some discretization uncertainties of our lattice

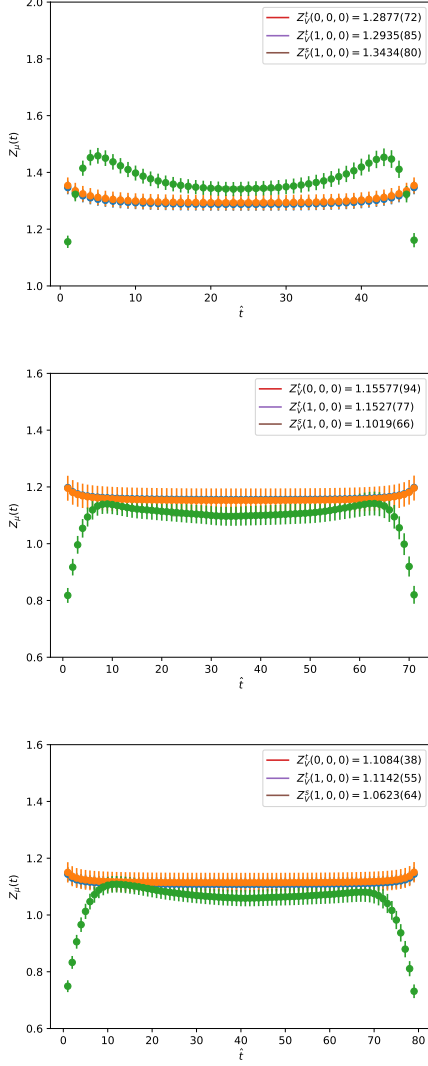


FIG. 1. The renormalization factor Z_V^μ with respect to t for the three lattices. From top to bottom corresponds to $\beta = 2.4, 2.8, 3.0$. The superscript t of Z_V denotes $\mu = 0$ and s denotes $\mu = 1, 2, 3$ corresponding to non-zero momentum direction.

setup. We will work in rest frame of the pseudoscalar (such as η_c) with J/ψ moving with a definite momentum $\hat{p}_i = 2\pi\hat{n}/La_s$, where \hat{n} ranges from $(0, 0, 0)$ to $(2, 2, 2)$. As mentioned above, both the three-point functions and two-point functions are required in order to extract the desired hadronic matrix elements of the current $J_\mu^{(\text{em})}$. We choose the quark bilinear operators $\mathcal{O}_i(x) = (\bar{c}\Gamma_i c)(x)$ for η_c ($\Gamma_i = \gamma_5$) and J/ψ ($\Gamma_i = \gamma_i, i = 1, 2, 3$), such that the two-point function with momentum \vec{p} can be calculated through

$$\Gamma_{ij}^{(2)}(\vec{p}, t) = - \sum_{\vec{x}} e^{-i\vec{p}\cdot\vec{x}} \text{Tr} \langle S^\dagger(\vec{x}, t; \mathbf{0}, 0) \Gamma_i S(\vec{x}, t; \mathbf{0}, 0) \Gamma_j \rangle \quad (9)$$

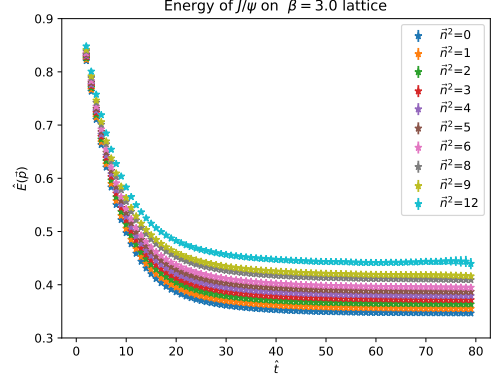


FIG. 2. Effective energy plateaus $E(\vec{p})$ of J/ψ for $\beta = 3.0$. $E(\vec{p})$ is the average over the momentum modes with the same $|\vec{p}|^2$. It is seen that signal-to-noise ratios are good for the momentum modes we are used.

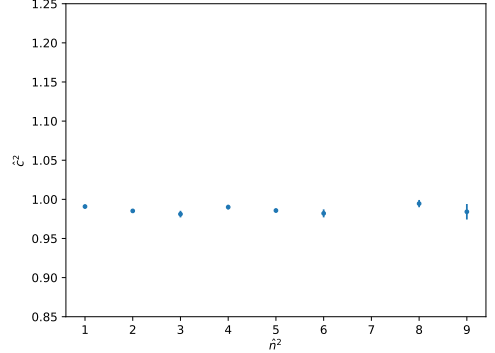


FIG. 3. The deviations of squared speed of light c^2 from one on $\beta = 3.0$ lattice. The same of \hat{n}^2 have been averaged where \hat{n} range from $(0, 0, 0)$ to $(2, 2, 2)$. The largest deviation of squared speed of light c^2 from one is less than 4% on all the three lattices.

where $S(\vec{x}, t, \vec{0}, 0)$ is the point-source propagator of the charm quark. In this work we ignore the quark annihilation diagrams. The effective energy plateaus $E(\mathbf{p})$ of J/ψ are illustrated in Fig. 6 for $\beta = 3.0$. We check the dispersion relation of J/ψ and find the largest deviation of squared speed of light c^2 from one is less than 4% on all the three lattices, as shown in Fig. 3, where c^2 is derived by

$$c^2 = \frac{E^2(\vec{p}) - m_{J/\psi}^2}{|\vec{p}|^2}. \quad (10)$$

The three-point functions $\Gamma_{J/\psi \rightarrow \gamma \eta_c}^{(3), \mu i}$ contributed by the connected diagrams (disconnected diagrams are ne-

glected) are calculated through the expression

$$\begin{aligned} \Gamma_{J/\psi \rightarrow \gamma \eta_c}^{(3), \mu i}(\vec{p}_i, t_i; \vec{p}_f, t_f; t) &= \sum_{\vec{x}, \vec{y}} e^{-i\vec{p} \cdot \vec{x} + i\vec{q} \cdot \vec{y}} \langle \mathcal{O}_5(\vec{x}, t_f) \\ &\quad \times (\bar{c} \gamma_\mu c)(\vec{y}, t) \mathcal{O}_i^\dagger(0) \rangle \\ &= - \sum_{\vec{y}} e^{i\vec{q} \cdot \vec{y}} \text{tr} \langle H_{\Gamma_f}^\dagger(\vec{y}, 0; t_f; \vec{p}_f) \\ &\quad \times \gamma_5 \gamma_\mu S(\vec{y}, 0) \gamma_i \rangle \end{aligned} \quad (11)$$

where

$$H_{\Gamma_f}(y, 0; t_f; \vec{p}) \equiv \sum_{\vec{x}} e^{i\vec{p} \cdot \vec{x}} S(\vec{y}, \vec{x}) \gamma_5 S(\vec{x}, 0) \gamma_5 \quad (12)$$

can be obtained by sequential source technique [20]. In order to increase the statistics, we repeat the same calculations T times (where T is the temporal lattice size) by setting a point source on a different time slice each time. With the related two-point functions calculated accordingly, a straightforward way to extract the interested matrix elements $\langle \eta_c(\vec{p}_f, \lambda_f) | J_{\text{em}}^\mu(0) | J/\psi(\vec{p}_i, \lambda_i) \rangle$ is to fit the three-point function and two-point function simultaneously according to Eq. (6) and Eq. (7) through the jackknife analysis. To suppress the contribution of excited states, we use this formula

$$\begin{aligned} R_{i, \mu, f}(t) &= \Gamma_{i, \mu, f}^{(3)}(\vec{p}_f, \vec{q}, t_f, t) \sqrt{\frac{2E_i \Gamma_i^{(2)}(\vec{p}_i, t_f - t)}{\Gamma_i^{(2)}(\vec{p}_i, t) \Gamma_i^{(2)}(\vec{p}_i, t_f)}} \\ &\quad \times \sqrt{\frac{2E_f \Gamma_f^{(2)}(\vec{p}_f, t)}{\Gamma_f^{(2)}(\vec{p}_i, t_f - t) \Gamma_i^{(2)}(\vec{p}_i, t_f)}} \end{aligned} \quad (13)$$

which gives flatter plateaus. In practice, the energies of $E_{i, f}$ are derived from two-point functions in the joint fit of the two-point and three-point functions. We can get the form factors by solving the Eq. (3). Based on the OZI rule, we neglect the contribution from the quark annihilation diagrams and only consider the contribution of connected diagrams. As such we compute the form factor $\hat{V}(Q^2)$ which is related to $V(Q^2)$ by

$$V(Q^2) = 2 \times \frac{2}{3} e \times \hat{V}(Q^2), \quad (14)$$

where the factor 2 comes from the insertion of the electromagnetic current to both the quark and antiquark lines, $2/3e$ is the electric charge of charm quark. In the expression above, the renormalization constant of the spatial component of $J_\mu^{(\text{em})}$, say, $Z_V^{(s)}$, has been implicitly incorporated into $\hat{V}(Q^2)$. The extracted $\hat{V}(Q^2)$ on the three lattices we are using are plotted in terms of Q^2 in Fig. 4. Maybe the lattice of $8^3 \times 96$ is too coarse, that would lead to poor fitting. We try to fit with the data of three small Q^2 , and $\hat{V}(Q^2)$ at 2.045(36) is gained. We regard the difference between the results fitted with different Q^2 range as systematic error. The errors on other two lattices are statistical errors.

TABLE III. The mass of J/ψ , η_c and the form factor $\hat{V}(0)$ on three lattices.

β	$m_{J/\psi}$ (GeV)	m_{η_c} (GeV)	$\hat{V}(0)$
2.4	3.097(1)	2.995(1)	2.152(34)(107)
2.8	3.102(1)	3.007(2)	1.962(14)
3.0	3.105(1)	2.995(1)	1.971(18)
∞			1.933(41)

In order to obtain the on-shell form factor $V(Q^2 = 0)$, we adopt the following function form to do the extrapolation,

$$\hat{V}(Q^2) = \hat{V}(0) e^{-\frac{Q^2}{16\beta^2}} \quad (15)$$

which is inspired by the simple quark model with the harmonic oscillator wavefunctions of η_c and J/ψ , as addressed in Ref. [20]. The extrapolations are also illustrated in Fig. 4 by curves with error bands. It is interesting to see that this kind of function form describes the data very well (On our coarsest lattice, there is a clear deviation from the curve, which is tentatively attributed to the relatively large discretization error of Q^2 calculated on the lattice). The results after the extrapolation are listed in Tab. III and shown in Fig. 5. Since we have three lattices with different lattice spacings a_s , we also perform a linear extrapolation

$$\hat{V}(0, a_s) = \hat{V}(0)^{\text{cont.}} + A a_s^2 \quad (16)$$

to get the final result of $\hat{V}(0)^{\text{cont.}}$,

$$\hat{V}(0)^{\text{cont.}} = 1.933(41), \quad (17)$$

from which we give the prediction of the partial width of the process $J/\psi \rightarrow \gamma \eta_c$,

$$\begin{aligned} \Gamma_{J/\psi \rightarrow \gamma \eta_c} &= \frac{\alpha |\vec{q}|^3}{(m_{J/\psi} + m_{\eta_c})^2} \frac{64}{27} |\hat{V}(0)|^2 \\ &= 2.47(11) \text{keV}, \end{aligned} \quad (18)$$

where the fine coupling constant takes the value at the charm quark mass scale, $\alpha = \frac{1}{134}$, and $m_{J/\psi}$ and m_{η_c} assume the experimental values.

We would like to compare our result with those from previous lattice QCD studies in Tab. IV where one can see that all the results reach a consensus within errors. This assures us that, in our study, the systematic uncertainties are not important in the charmonium sector.

B. The partial decay width of J/ψ radiatively decaying into the pseudoscalar glueball

We extend the similar study to the process of J/ψ radiatively decaying into the pseudoscalar glueball. It is known that the signals of glueballs are always noisy, such that a large statistics is required. On the other hand, an

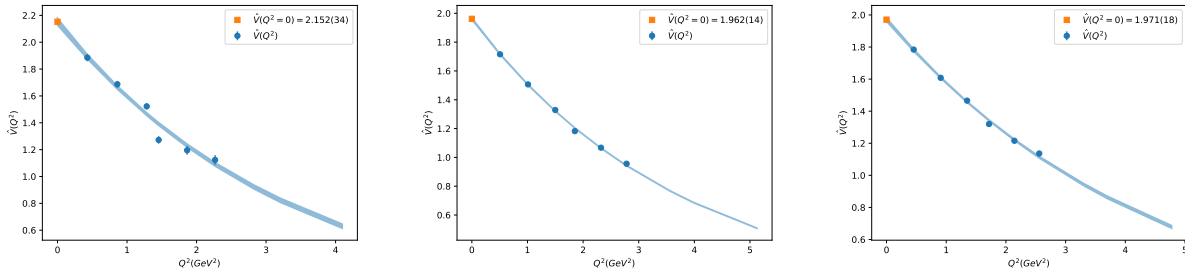


FIG. 4. The form factor $V(Q^2)$ in Eq. (3) of J/ψ to $\gamma\eta_c$ where $Q^2 = -(P_{J/\psi} - P_{\eta_c})^2$. Exponential functions in Eq. 15 are adopted for extrapolation. From left to right corresponds to $\beta = 2.4, 2.8, 3.0$ lattices.

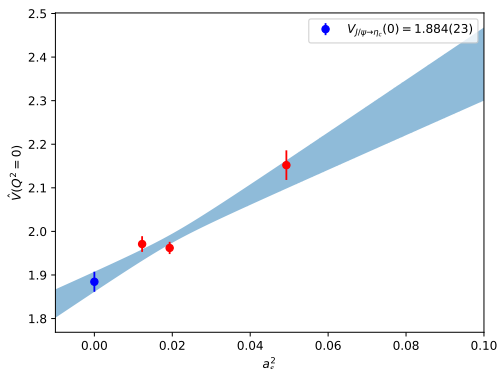


FIG. 5. The continuum extrapolation of form factor $V(Q^2)$ of $J/\psi \rightarrow \gamma\eta_c$ on three lattices. The lattice spacing a_s is in physical units, fm . The linear function are adopted for extrapolation.

TABLE IV. Comparison of $V(\hat{0})$ with previous lattice results

Lattice setup	$\hat{V}(0)$
$N_f = 2 + 1$ [21]	1.90(7)(1)
$N_f = 2$ [22]	1.92(3)(2)
$N_f = 2$ [23]	2.01(2)
Quenched [20]	1.85(4)
Quenched (this work)	1.933(41)

optimal interpolation operator, which couples predominantly to the ground state $|G\rangle$ of the pseudoscalar glueball, is mandatory for us to extract the desired matrix element $\langle G | J_\mu^{\text{em}}(0) | J/\psi \rangle$ reliably from the related three-point functions in Eq. (6). In doing so, we adopt the strategy used in [1, 2] to construct the optimal glueball operators, which is outlined as follows. First, the last four of the ten Wilson loops in Fig. 3 of Ref. [2] are used as prototypes, and then six smearing schemes (different combinations of the single-like smearing and the double-link smearing, as addressed in Ref. [1]) are applied to each of these prototype loops. Thus we obtain 24 different Wilson loops as the basis operators. Since

the lattice counterpart of the quantum number 0^{-+} in the continuum is A_1^{-+} , where A_1 is one of the five irreducible representations A_1, A_2, E, T_1, T_2 of the spatial symmetry group O of the cubic lattice, we apply the 24 operations of O group to each of the basis operators and obtain 24 copies of it, whose proper linear combination gives the representation of A_1^{-+} . Thereby we get 24 different operators with the quantum number A_1^{-+} , which compose a operator set $\{\phi_\alpha, \alpha = 1, 2, \dots, 24\}$. Based on this operator set, we calculate the matrix of the correlation functions $\tilde{C}(t) = \{\tilde{C}_{\alpha\beta}\}$ with

$$\tilde{C}_{\alpha\beta}(t) = \frac{1}{N_t} \sum_{\tau} \langle 0 | \phi_\alpha(t + \tau) \phi_\beta(\tau) | 0 \rangle \quad (19)$$

where we sum over τ to increase the statistics. Finally, by solving the generalized eigenvalue problem

$$\tilde{C}^{(i)}(t_D)V = \lambda(t_D)\tilde{C}^{(i)}(0)V, \quad (20)$$

we can get the eigenvector $V = \{v_\alpha, \alpha = 1, 2, \dots, 24\}$ corresponding to the maximal eigenvalue $\lambda_{\text{max}}(t_D) \equiv e^{-m_{\text{min}}(t_D)t_D}$ ($m_{\text{min}}(t_D)$ is close to the mass of the ground state), from which we can obtain the optimal operator $\Phi(t)$ for the ground state pseudoscalar glueball $|G\rangle$ by the combination $\Phi(t) = \sum_{\alpha} v_{\alpha} \phi_{\alpha}$. In this work, we set $t_D = 1$. The correlation function of $\Phi(t)$ can be parameterized as

$$C(t) = \frac{1}{T} \sum_{\tau} \langle \Phi(t + \tau) \Phi^\dagger(\tau) \rangle \simeq \frac{Z_G^2}{2m_G V_3} e^{-m_G t} = W e^{-m_G t}, \quad (21)$$

where m_G is the mass of the ground state, $V_3 = L^3 a_s^3$ is the spatial volume of the lattice, and $Z_G = |\langle 0 | \Phi(0) | G \rangle|$. The effective mass of $C(t)$ is plotted in Fig. 6, where one can see that the plateau almost starts from the beginning of time t . Obviously, there is still some contribution from higher states which manifests by the slight increment of the effective mass toward $t = 0$. To check the extent of the higher state contamination, we fit $C(t)$ through a single-exponential function and find that the deviation of W from one is at a level of few percents (note

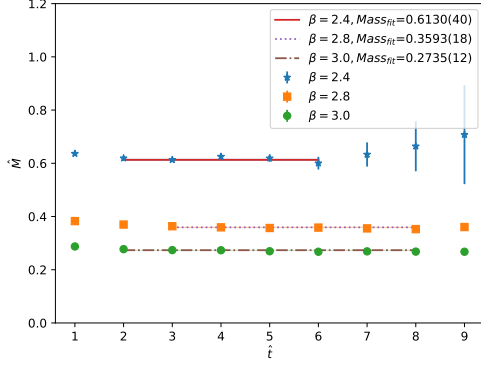


FIG. 6. The effect mass of pseudoscalar glueball extracted from the two-point correlation function which constructed by optimal glue operators on three lattices.

that $C(t)$ is normalized as $C(0) = 1$. This means that $C(t)$ is almost totally dominated by the contribution from the ground state and therefore $W \simeq 1$, or equivalently, $Z_G \simeq \sqrt{2m_G V_3}$ can be a good approximation. The mass of the ground state pseudoscalar glueball on the three lattices are listed in Tab. V. We obtain the mass of pseudoscalar glueball as 2.395(14) GeV after continuum extrapolation. This value is lower than that in Ref. [2], but it is consistent within the error-bar.

With the optimal operator $\Phi(t)$, the relevant three-point function can be calculated and parameterized as

$$\begin{aligned} \Gamma_{J/\psi \rightarrow \gamma G_{ps}}^{(3), i\mu} &= \frac{1}{T} \sum_{\tau, \vec{y}} e^{-i\vec{q} \cdot \vec{y}} \langle \Phi(t_f + \tau) J_\mu(\vec{y}, t + \tau) \mathcal{O}_{V,i}(\vec{0}, \tau) \rangle \\ &\simeq \sum_{V,r} \frac{e^{-m_G(t_f-t)} e^{-E_V t}}{2m_G V_3 2E_V(\vec{p}_i)} \langle 0 | \Phi(0) | G \rangle \\ &\quad \times \langle V(\vec{p}_i, r) | \mathcal{O}_{V,i}^\dagger(0) | 0 \rangle \langle G | J_\mu(0) | V(\vec{p}_i, r) \rangle. \quad (22) \end{aligned}$$

Similar to the case of J/ψ to $\eta_c \gamma$, we use this formula

$$\begin{aligned} R_{i,\mu,f}(\vec{q}, t) &= \Gamma^{(3), \mu}(\vec{q}, t_f, t) \frac{\sqrt{4V_3 m_{ps} E_{J/\psi}(\vec{q})}}{C(t_f - t)} \\ &\quad \times \sqrt{\frac{\Gamma_{J/\psi}^{(2)}(\vec{q}, t_f - t)}{\Gamma_{J/\psi}^{(2)}(\vec{q}, t) \Gamma_{J/\psi}^{(2)}(\vec{q}, t_f)}} \quad (23) \end{aligned}$$

to extract the matrix elements $\langle G_{ps} | J_\mu | J/\psi \rangle$, through which the contribution from excited states can be suppressed to some extent.

We fix the time interval of glueball operator and vector current operator as one time slice which mean $t_f - t = 1$, since that the optimal glueball operator projects almost totally on the ground state pseudoscalar glueball. Using the same multipole decomposition formula as $J/\psi \rightarrow \gamma \eta_c$, the transition width of $J/\psi \rightarrow \gamma G_{ps}$ is

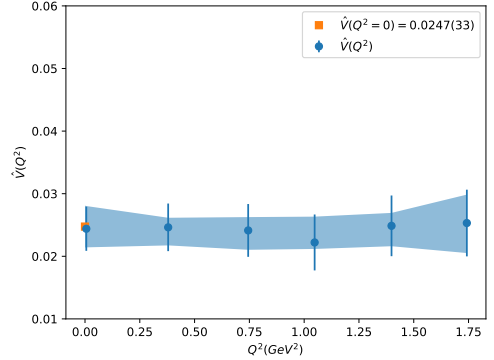
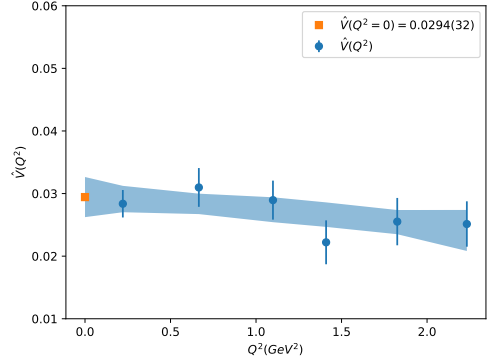
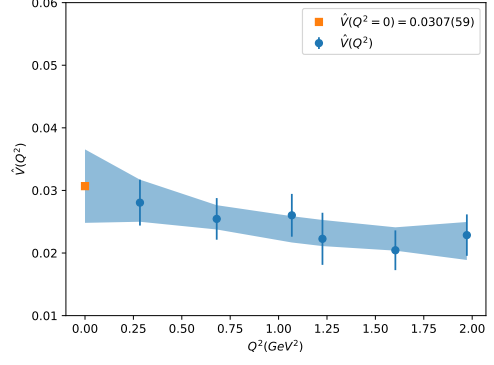


FIG. 7. The form factor $M_1(Q)$ and the extrapolated value $M_1(Q^2 = 0)$ of $J/\psi \rightarrow \gamma G_{ps}$ where $Q^2 = -(P_{J/\psi} - P_{G_{ps}})^2$. We adopted the function $F(Q^2 = 0) + a * Q^2 + b * Q^4$ to perform extrapolation.

$$\Gamma(J/\psi \rightarrow \gamma G_{ps}) = \frac{16}{27} \alpha \frac{|\vec{q}|^3}{(m_{ps} + m_{J/\psi})^2} |\hat{V}(0)|^2 \quad (24)$$

where $\hat{V}_G(0)$ denotes the form factor of $J/\psi \rightarrow \gamma G_{ps}$ which could be calculated on $Q^2 \neq 0$ and need be extrapolated to $Q^2 = 0$, and m_{ps} is the pseudoscalar glueball mass using the extrapolated value from three lattice results. The three-point function are calculated by setting the pseudoscalar glueball at rest and the J/ψ moving. The form factor $\hat{V}_G(Q^2)$ with various Q^2 are plotted in

TABLE V. The mass of pseudoscalar glueball and the form-factor $\hat{V}(0)$ of $J/\psi \rightarrow \gamma G_{ps}$. The function 25 has been adopted to perform extrapolation.

β	m_G (GeV)	$\hat{V}(0)$
2.4	2.724(18)	0.0307(59)
2.8	2.550(13)	0.0294(32)
3.0	2.464(11)	0.0247(33)
Continuum limit	2.395(14)	0.0246(43)
	2.560(35)(120)[2]	

Fig. 7 and be extrapolated to $Q^2 = 0$ by the formula

$$\hat{V}(Q^2) = \hat{V}(0) + aQ^2 + bQ^4. \quad (25)$$

After extrapolating to the physical limit by

$$\hat{V}(0) = \hat{V}(0)^{cont.}.$$

we get the final result as

$$\hat{V}(0)^{cont.} = 0.0246(43) \quad (26)$$

also plotted in Fig. 8. Finally we give the decay width of $J/\psi \rightarrow \gamma G_{ps}$ is

$$\Gamma(J/\psi \rightarrow \gamma G_{ps}) = \begin{cases} 0.0215(74) \text{ keV} & M_{G_{ps}} = 2.395 \\ 0.0099(34) \text{ keV} & M_{G_{ps}} = 2.56 \end{cases} \quad (27)$$

which gives the production fraction of the pseudoscalar glueball

$$Br(J/\psi \rightarrow \gamma G) = \begin{cases} 2.31(80) \times 10^{-4} & M_{G_{ps}} = 2.395 \\ 1.07(37) \times 10^{-4} & M_{G_{ps}} = 2.56 \end{cases}. \quad (28)$$

IV. DISCUSSION

Obviously, production fraction of the pure gauge pseudoscalar glueball is quite small in the J/ψ radiative decays, especially when comparing with $3.8(9) \times 10^{-3}$ of the pure gauge scalar glueball and roughly 1% of the tensor glueball. Furthermore, this value is also much smaller than those of most known pseudoscalars. For example, the branching fraction of $J/\psi \rightarrow \gamma \eta'$ is $5.13(17) \times 10^{-3}$, which is one orders of magnitude larger. One of the reasons is that J/ψ radiatively decaying into a pseudoscalar X is through the $M1$ decay, such that the partial width is proportional to $|\vec{q}|^3$ with $|\vec{q}| = (m_{J/\psi}^2 - m_X^2)/(2m_{J/\psi})$ being the magnitude of the decaying momentum of the final state photon. Because the mass 2.4 GeV of the pseudoscalar glueball is close to the mass of J/ψ , the partial

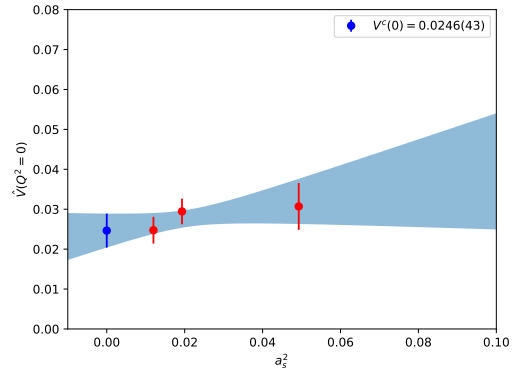


FIG. 8. The continuum extrapolation of the form-factor $V(Q^2 = 0)$ of $J/\psi \rightarrow \gamma G_{ps}$. The result show that the form-factor $V(0)$ is very weak dependence to lattice spacing.

width is suppressed by the kinematics. In order to obtain a fair comparison, we would like to subtract the phase space factor and introduce an effective coupling g_X through the definition

$$\Gamma(J/\psi \rightarrow \gamma X) = \frac{1}{3} \alpha g_X^2 \frac{|\vec{q}|^3}{m_{J/\psi}^2}, \quad (29)$$

where $1/3$ accounts for the spin average of the J/ψ , α is the fine coupling constant. Obviously, g_X describes the coupling of the gluons generated through $c\bar{c}$ annihilation to the pseudoscalar meson X . Since in experiments only the branching fractions $Br(J/\psi \rightarrow \gamma X)$ can be measured directly, we express g_X explicitly in terms of these branching fractions along with the total width $\Gamma_{J/\psi}$ as

$$g_X = \left[\frac{24\Gamma_{J/\psi} Br(J/\psi \rightarrow \gamma X) m_{J/\psi}^5}{\alpha (m_{J/\psi}^2 - m_X^2)^3} \right]^{\frac{1}{2}}. \quad (30)$$

In practice, for η , η' , and $\eta(2225)$, we take the branch fractions directly from the PDG data. For $\eta(1405)$ and $\eta(1475)$, their production rates in the J/ψ decays are not differentiated from each other in PDG, so we also take them as a whole and sum over the branching fractions of final states $\gamma K \bar{K} \pi$, $\gamma \gamma \rho$, $\gamma \eta \pi^+ \pi^-$, and $\gamma \rho^0 \rho^0$. For $\eta(1760)$ we add up the branching fractions of $\gamma \rho^0 \rho^0$ and $\gamma \omega \omega$, for $X(1835)$ we add use the sum of the branching ratios of the final states $\gamma + (\pi^+ \pi^- \eta', p \bar{p}, \eta K_S K_S)$. The derived g_X 's are listed in Tab. VII.

The striking observation is that the coupling g_X for the pseudoscalar glueball is comparable with or smaller than those of the known non-flavored pseudoscalars (note that the smallness of g_η is due to the dominance of the flavor octet component of $\eta(547)$). This is in sharp contrast to the usual expectation based on the naive α_s -power counting that the gluons in the J/ψ radiative decay couple more strongly to glueballs than $q\bar{q}$ mesons. Even though this naive α_s -power counting is not justified in the low energy QCD regime, empirically there is an OZI rule

TABLE VI. The branch fractions of J/ψ radiative decay to pseudoscalar light mesons from the PDG data[24].

pseudoscalar mesons	final states	branching ratios
η	$\gamma\eta$	$(1.104 \pm 0.034) \times 10^{-3}$
η'	$\gamma\eta'$	$(5.13 \pm 0.17) \times 10^{-3}$
$\eta(1405/1475)$	$\gamma\eta(1405/1475) \rightarrow \gamma K \bar{K} \pi$	$(2.8 \pm 0.6) \times 10^{-3}$
	$\gamma\eta(1405/1475) \rightarrow \gamma\gamma\rho^0$	$(7.8 \pm 2.0) \times 10^{-5}$
	$\gamma\eta(1405/1475) \rightarrow \gamma\eta\pi^+\pi^-$	$(3.0 \pm 0.5) \times 10^{-4}$
	$\gamma\eta(1405/1475) \rightarrow \gamma\rho^0\rho^0$	$(1.7 \pm 0.4) \times 10^{-3}$
$\eta(1760)$	$\gamma\eta(1760) \rightarrow \gamma\rho^0\rho^0$	$(1.3 \pm 0.9) \times 10^{-4}$
	$\gamma\eta(1760) \rightarrow \gamma\omega\omega$	$(1.98 \pm 0.33) \times 10^{-3}$
$X(1835)$	$\gamma X(1835) \rightarrow \gamma\pi^+\pi^-\eta'$	$(2.77_{-0.40}^{+0.34}) \times 10^{-4}$
	$\gamma X(1835) \rightarrow \gamma p\bar{p}$	$(7.7_{-0.9}^{+1.5}) \times 10^{-5}$
	$\gamma X(1835) \rightarrow \gamma K_S^0 K_S^0 \eta$	$(3.3_{-1.3}^{+2.0}) \times 10^{-5}$
$\eta(2225)$	$\gamma\eta(2225)$	$(3.14_{-0.19}^{+0.50}) \times 10^{-4}$

TABLE VII. The g_X of flavor-singlet pseudoscalar mesons.

Pseudoscalar (X)	g_X
η	0.0108(2)
η'	0.0259(8)
$\eta(1405/1475)$	0.0313(41)
$\eta(1760)$	0.0255(25)
$X(1835)$	0.0123(12)
$\eta(2225)$	0.0167(17)
$G(0^{-+})$	0.0126(22)

observed in many hadronic processes that the processes mediated through gluons, say, involving the Feynman diagrams without continuous quark lines connecting the initial and final states, tend to be strongly suppressed.

In this sense, the production of η states in the J/ψ radiative decays seems to be OZI-violated. The QCD chiral anomaly may play an important role in these processes. In QCD, the flavor singlet axial vector current

$$j_5^\mu(x) = \sum_{k=1}^{N_f} 2im_k \bar{q}_k(x) \gamma_5 \gamma^\mu q_k(x)$$

is not conserved,

$$\partial_\mu j_5^\mu(x) = 2N_f q(x) + \sum_{k=1}^{N_f} 2im_k \bar{q}_k(x) \gamma_5 q_k(x), \quad (31)$$

even in the chiral limit $m_k \rightarrow 0$, where N_f is the number of the quark flavor, and the anomalous gluonic term $q(x) = \frac{g^2}{16\pi^2} \text{tr} G_{\mu\nu}(x) \tilde{G}^{\mu\nu}(x)$ comes either from the regularization of the linearly divergent one-loop diagrams of the vector-vector-axial vector current vertex (the triangle diagram) in the perturbation theory or the chiral transformation non-invariance of the fermion measure in the path integral formalism. As shown in Ref. [25, 26], the matrix element related to the chiral anomaly can be sizeable, and obviously violated the OZI rule. In other words, the QCD $U_A(1)$ anomaly can enhance the coupling of η states to gluons, and this non-perturbative effect results in the violation of the OZI rule when flavor singlet pseudoscalar mesons are involved.

There is also evidence from lattice QCD study that the topological charge density $q(x)$ couples to η' strongly. A $N_f = 2 + 1$ lattice simulation uses $q(x)$ to study η' and observes a clear contribution of η' to the correlation function $\langle q(x)q(0) \rangle$ [27]. The authors get the result $m_{\eta'} = 1019(119)$ MeV at the physical pion mass consistent with the physical η' mass. Similar lattice studies have also been carried out in the $N_f = 2$ case [8, 28]. In Ref. [8], the authors get the mass of the isoscalar pseudoscalar η_2 to be $m_{\eta_2} = 890(38)$ MeV at $m_\pi = 650$ MeV. In Ref. [28], the authors use both the fermionic operator $\bar{\psi}\gamma_5\psi$ and $q(x)$, and get compatible results for m_{η_2} on several gauge ensembles, whose chiral extrapolation gives $m_{\eta_2} = 772(18)$ MeV.

The discussion above helps to understand why the couplings of gluons to η states are not suppressed in comparison with the coupling of the pseudoscalar glueball in the J/ψ radiative decays. This also implies the coupling g_X cannot be used as a characteristics for identifying the pseudoscalar glueball. Anyway, since the lattice QCD studies predicts the pseudoscalar glueball mass is around 2.4-2.6 GeV, we may wish to check if there are any candidates in this mass region. With the world largest J/ψ event ensemble, the BESIII Collaboration is performing a scrutinized partial wave analysis on the radiative J/ψ decay processes. In the process $J/\psi \rightarrow \gamma\eta'\pi^+\pi^-$, BESIII observes resonance-like structure $X(2120)$ and $X(2370)$ in the invariant mass spectrum of $\eta'\pi^+\pi^-$ [16, 29], however, their spin and parity have not been determined yet. $X(2370)$ is confirmed in the invariant mass spectra of $\eta'K\bar{K}$ by BESIII [30], and its production fractions in the processes $J/\psi \rightarrow \gamma X(2370) \rightarrow \gamma\eta'K^+K^-$ and $J/\psi \rightarrow \gamma X(2370) \rightarrow \gamma\eta'K_S K_S$ have been estimated to be $[1.86 \pm 0.39(sta.) \pm 0.29(syssa.)] \times 10^{-5}$ and $[1.19 \pm 0.37(sta.) \pm 0.18(syssa.)] \times 10^{-5}$, respectively. In the partial wave analysis of the process $J/\psi \rightarrow \gamma\phi\phi$, BESIII also observes a component $X(2500)$, whose preferred spin-parity assignment is pseudoscalar [15]. Its production fraction in the process $J/\psi \rightarrow \gamma X(2500) \rightarrow \gamma\phi\phi$ is determined to be $[1.7 \pm 0.2_{-0.8}^{+0.2}] \times 10^{-5}$. Whether they are

the same object or not, $X(2370)$ and $X(2500)$ reside in the pseudoscalar glueball mass region predicted by lattice QCD, whose production rates are compatible with that of the pseudoscalar glueball in this work. Recently, BESIII has finished the data collection of 10 billion J/ψ events, hopefully the properties of these states can be determined more precisely in the near future.

V. SUMMARY

We carry out the first lattice calculation of the production rate of the pseudoscalar glueball in J/ψ radiative decays in the quenched approximation. We generate gauge configurations on three anisotropic lattices with different lattice spacings, which facilitate us to perform the continuum limit extrapolation. In order to calibrate some of the systematic uncertainties, we first calculate partial decay width of $J/\psi \rightarrow \gamma\eta_c$. The related M_1 transition form factor is determined to be $\hat{V}(0) = 1.933(41)$, which gives the partial width $\Gamma(J/\psi \rightarrow \gamma\eta_c) = 2.47(11)$ keV. These results are consistent with the results of previous lattice calculations.

By applying the variational method to a large operator set, we obtain an optimal operator which couples predominantly to the ground state pseudoscalar glueball G . In this work, m_G is determined to be 2.395(14) GeV, and the on-shell form factor of $J/\psi \rightarrow \gamma G$ is derived as $\hat{V}(0) = 0.0246(43)$, in the continuum limit, from which we obtain the following partial decay width and the production rate

$$\begin{aligned}\Gamma(J/\psi \rightarrow \gamma G) &= 0.0215(74) \text{ keV} \\ Br(J/\psi \rightarrow \gamma G) &= 2.31(80) \times 10^{-4}\end{aligned}\quad (32)$$

We introduce an effective coupling g_X to describe the interaction between the pseudoscalar X and the gluonic intermediate states in the processes $J/\psi \rightarrow \gamma X$, as defined in Eq. (30). It is interesting to see that all the g_X 's are comparable for the pseudoscalar glueball and the non-flavored $q\bar{q}$ pseudoscalars (η states). We tentatively attribute the large production rates of the η states to the QCD $U_A(1)$ anomaly which is totally a nonperturbative effect.

Even though this study is performed in the quenched approximation and the uncertainty in the presence of dynamical quarks is not controlled, we hope our result can provide useful theoretical information for experiments to unravel the properties of the possible pseudoscalar glueball.

ACKNOWLEDGEMENTS

L.C. thanks J. Liang for useful discussions. This work is supported by the National Key Research and Development Program of China (No.2017YFB0203202). The numerical calculations are carried out on Tianhe-1A at the National Supercomputer Center (NSCC) in Tianjin and the GPU cluster at Hunan Normal University. We acknowledge the support of the National Science Foundation of China (NSFC) under Grants No. 11575196, No. 11405053, No. 11335001 and No. 11621131001 (CRC 110 by DFG and NSFC). Y.C. is also supported by the CAS Center for Excellence in Particle Physics (CCEPP) and National Basic Research Program of China (973 Program) under code number 2015CB856700. Y.Y. is supported by the CAS Pioneer Hundred Talents Program. Our matrix inversion code is based on QUDA libraries[31] and the fitting code is based on lsqfit[32].

-
- [1] C. Morningstar and M. Peardon, *Phys. Rev. D* **60**, 34509 (1999), [arXiv:9901004 \[hep-lat\]](#).
 - [2] Y. Chen, A. Alexandru, S. J. Dong, T. Draper, I. Horváth, F. X. Lee, K. F. Liu, N. Mathur, C. Morningstar, M. Peardon, S. Tamhankar, B. L. Young, and J. B. Zhang, *Phys. Rev. D* **73**, 014516 (2006), [arXiv:0510074 \[hep-lat\]](#).
 - [3] S. Nussinov and R. Shrock, *Phys. Rev. D* **80**, 054003 (2009), [arXiv:0907.1577 \[hep-ph\]](#).
 - [4] C. M. Richards, A. C. Irving, E. B. Gregory, and C. McNeile, *Phys. Rev. D* **82**, 34501 (2010), [arXiv:1005.2473v2](#).
 - [5] E. Gregory, A. Irving, B. Lucini, C. McNeile, A. Rago, C. Richards, and E. Rinaldi, *J. High Energy Phys.* **2012**, 0 (2012), [arXiv:1208.1858](#).
 - [6] W. I. Eshraim, S. Janowski, F. Giacosa, and D. H. Rischke, *Phys. Rev. D* **87**, 054036 (2013).
 - [7] C.-F. Qiao and L. Tang, *Phys. Rev. Lett.* **113**, 221601 (2014), [arXiv:1408.3995 \[hep-ph\]](#).
 - [8] W. Sun, L.-C. Gui, Y. Chen, M. Gong, C. Liu, Y.-B. Liu, Z. Liu, J.-P. Ma, and J.-B. Zhang, *Chinese Phys. C* **42**, 093103 (2017), [arXiv:1702.08174](#).
 - [9] L. Olbrich, M. Zétényi, F. Giacosa, and D. H. Rischke, *Phys. Rev. D* **97**, 014007 (2018).
 - [10] E. Klempt and A. Zaitsev, *Phys. Rept.* **454**, 1 (2007), [arXiv:0708.4016 \[hep-ph\]](#).
 - [11] W. Ochs, *J. Phys.* **G40**, 043001 (2013), [arXiv:1301.5183 \[hep-ph\]](#).
 - [12] W. Qin, Q. Zhao, and X.-H. Zhong, *Phys. Rev. D* **97**, 096002 (2018), [arXiv:1712.02550](#).

- [13] L. C. Gui, Y. Chen, G. Li, C. Liu, Y. B. Liu, J. P. Ma, Y. B. Yang, and J. B. Zhang, *Phys. Rev. Lett.* **110**, 021601 (2013), [arXiv:1206.0125](#).
- [14] Y. B. Yang, L. C. Gui, Y. Chen, C. Liu, Y. B. Liu, J. P. Ma, and J. B. Zhang, *Phys. Rev. Lett.* **111**, 091601 (2013), [arXiv:1304.3807](#).
- [15] M. Ablikim *et al.* (BESIII Collaboration), *Phys. Rev. D* **93**, 112011 (2016), [arXiv:1602.01523 \[hep-ex\]](#).
- [16] A. M. *et al.* (BESIII Collaboration), *Phys. Rev. Lett.* **106**, 072002 (2010), [arXiv:1012.3510](#).
- [17] C. Morningstar and M. Peardon, *Phys. Rev. D* **56**, 4043 (1997), [arXiv:9704011 \[hep-lat\]](#).
- [18] C. Liu, J. Zhang, Y. Chen, and J. Ma, *Nucl. Phys. B* **624**, 360 (2002).
- [19] J. Zhang and C. Liu, *Mod. Phys. Lett. A* **16**, 1841 (2001), [arXiv:0107005 \[hep-lat\]](#).
- [20] J. J. Dudek, R. G. Edwards, and D. G. Richards, *Phys. Rev. D* **73**, 74507 (2006), [arXiv:0601137 \[hep-ph\]](#).
- [21] G. C. Donald, C. T. H. Davies, R. J. Dowdall, E. Follana, K. Hornbostel, J. Koponen, G. P. Lepage, and C. McNeile, *Phys. Rev. D* **86**, 94501 (2012), [arXiv:1208.2855](#).
- [22] D. Becirevic and F. Sanfilippo, *J. High Energy Phys.* **2013**, 28 (2012), [arXiv:1206.1445](#).
- [23] Y. Chen, D.-C. Du, B.-Z. Guo, N. Li, C. Liu, H. Liu, Y.-B. Liu, J.-P. Ma, X.-F. Meng, Z.-Y. Niu, and J.-B. Zhang, *Phys. Rev. D* **84**, 34503 (2011), [arXiv:1104.2655](#).
- [24] M. Tanabashi *et al.* (Particle Data Group), *Phys. Rev. D* **98**, 030001 (2018).
- [25] M. Gong, Y.-B. Yang, J. Liang, A. Alexandru, T. Draper, and K.-F. Liu (χ QCD Collaboration), *Phys. Rev. D* **95**, 114509 (2017).
- [26] Y.-B. Yang (χ QCD), in *Proceedings, 36th International Symposium on Lattice Field Theory (Lattice 2018): East Lansing, MI, United States, July 22-28, 2018*, Vol. LATTICE2018 (2019) p. 017, [arXiv:1904.04138 \[hep-lat\]](#).
- [27] H. Fukaya, S. Aoki, G. Cossu, S. Hashimoto, T. Kaneko, and J. Noaki, *Phys. Rev. D* **92**, 1 (2015).
- [28] P. Dimopoulos, C. Helmes, C. Jost, B. Knippschild, B. Kostrzewa, L. Liu, K. Ottnad, M. Petschlies, C. Urbach, U. Wenger, and M. Werner, *Phys. Rev. D* **99**, 34511 (2019).
- [29] M. Ablikim *et al.* (BESIII Collaboration), *Phys. Rev. Lett.* **117**, 1 (2016), [arXiv:1603.09653v1](#).
- [30] V. Prasad, in *16th Conf. Flavor Phys. CP Viol.* (2018) [arXiv:1810.00180 \[hep-ex\]](#).
- [31] M. Clark, R. Babich, K. Barros, R. Brower, and C. Rebbi, *Comput. Phys. Commun.* **181**, 1517 (2010), [arXiv:0911.3191](#).
- [32] G. P. Lepage, B. Clark, C. T. H. Davies, K. Hornbostel, P. B. Mackenzie, C. Morningstar, and H. Trotter, *Nucl. Phys. Proc. Suppl.* **106**, 12 (2002), [arXiv:hep-lat/0110175 \[hep-lat\]](#).